Available online at www.sciencedirect.com
SCIENCE DIRECT®
Polymer 44 (2003) 7533–7538
polymer
www.elsevier.com/locate/polymer

Thermal stability and flammability of polyamide 66/montmorillonite nanocomposites

Huaili Qin[a], Quansheng Su[b], Shimin Zhang[a,*], Bin Zhao[a], Mingshu Yang[a]

[a]*State Key Laboratory of Engineering Plastics, Center for Molecular Science, Institute of Chemistry, P.O. Box 2709, Beijing 100080, People's Republic of China*
[b]*CNPC Liaoyang Petrochemical Fibre Co., Liaoyang, Liaoning 111003, People's Republic of China*

Received 14 May 2003; received in revised form 6 August 2003; accepted 12 September 2003

Abstract

Exfoliated nanocomposites based on polyamide 66 (PA66) and montmorillonite (MMT) were prepared and their thermal stability and combustion behaviour were investigated by using thermal gravity analysis and cone calorimeter. The nanocomposites exhibit higher thermal stability and good flame retardancy. The catalytic decomposition effect of MMT and the barrier effect of layer silicates are presented directly in isothermal oxidation experiment. The initial heat release rate plots show that the addition of MMT can accelerate the ignition of PA66 matrix. A ceramic-like char forms in the surface of the nanocomposites during burning. It is characterized by attenuated total reflection infrared spectra and scanning electron microscopy.

Keywords: PA66/MMT nanocomposite; Thermal stability; Flammability; Char

1. Introduction

In the past decade, polymer layered silicate nanocomposites (PLSN) have received considerable attention whether in fundamental research or industry exploitation [1–3]. Compared to conventional filled polymers, PLSN have a lot of unique properties in the presence of a small amount of silicate, such as enhanced mechanical properties, increased heat distortion temperature, improved thermal stability, decreased gas/vapour permeability and reduced flammability [4,5].

The cone calorimetry is one of the most effective bench-scale methods for studying the flammability properties of materials [6]. The cone calorimetric data show that the peak heat release rate (HRR) is reduced a lot in PLSN with involved matrices of polyamide 6 [7,8], polystyrene [9], polypropylene [6] and poly(ethylene-co-vinyl acetate) [10]. Moreover, it does not have the usual drawbacks associated with other fire retardant additives. It pioneers in development of flame-retarded polymeric materials, which is commended as a revolutionary new flame retardant approach [7]. The general view of the flame retardant mechanism is that a high-performance carbonaceous silicate char builds up on the surface during burning; this insulates the underlying material and slows the mass loss rate (MLR) of decomposition products [6].

Polyamide 66 (PA66) is an important synthetic resin and widely used in engineering plastics and fibre industries. It is flammable and thus anti-flaming modification is necessary in many cases of usage. In this paper, we investigated the thermal stability and combustion behaviour of PA66/MMT nanocomposites through thermal gravity analysis (TGA) and cone calorimeter. The nanocomposites were produced by the melting intercalation technique and their nanostructure was characterized by transmission electron microscopy (TEM) and X-ray diffraction (XRD). The carbonaceous silicate char that builds up on the surface from the start before ignition in the cone calorimetric experiment was characterized by attenuated total reflection infrared (ATR-IR) spectra and scanning electron microscopy (SEM).

* Corresponding author. Tel.: +86-10-82615665; fax: +86-10-62559373.
E-mail address: smzhang@sklep.icas.ac.cn (S.M. Zhang).

0032-3861/$ - see front matter © 2003 Elsevier Ltd. All rights reserved.
doi:10.1016/j.polymer.2003.09.014

2. Experimental

2.1. Materials

The PA66 (viscosity average molecular weight 1.67×10^4) was supplied by CNPC Liaoyang Petrochemical Fibre Co., Liaoyang, China. The inorganic montmorillonite (MMT), with interlayer cation of Na^+ and having a cation exchange capacity (CEC) of 90 meq/100 g, was purchased from Qinghe Chemical Factory, Zhangjiakou, China. The organophilic MMT (OMMT) was prepared via cation-exchange reaction using alkylammonium.

2.2. Preparation

The PA66/MMT composites were obtained by compounding the polymer with 2, 5, and 10 wt% of OMMT and 5 wt% of MMT in a twin-screw extruder (Nanjing Rubber and Plastics Machinery Plant, SHJ30, $L/\Phi = 23$). The temperature of the extruder was maintained at 250, 260, 265, and 260 °C from hopper to die, respectively. The composites are denoted hereafter OMMT-2, OMMT-5, OMMT-10 and MMT-5, respectively. The dried pellets of the composites were injection moulded into $100 \times 100 \times 10$ mm^3 specimens. Samples of pure polymer were processed in the same way and used for comparison.

2.3. Morphological characterization

X-ray diffraction (XRD) patterns were obtained using a Rigaku D/max 2400 diffractometer with Cu Kα radiation ($\lambda = 0.154$ nm, 40 kV, 120 mA) at room temperature, the diffractograms were scanned from 1.5 to 40° in the 2θ range in 0.02° steps, scanning rate was 8°/min.

The morphology structure of the composites was investigated by a Hitachi (Japan) H-800 transmission electron microscope (TEM) with an acceleration voltage of 100 kV. The ultrathin slides were obtained by sectioning the injection-moulded samples along the direction perpendicular to the injection.

2.4. TGA characterization

The thermal stability was measured by thermogravimetry (TGA; Perkin–Elmer 7 series; Perkin–Elmer Cetus Instruments, Norwalk, CT), with a heating ramp of 20 °C/min in nitrogen or air atmospheres and in isothermal conditions at 360 °C in air.

2.5. Cone calorimetric characterization

Combustion experiments were performed in a cone calorimeter (Fire Testing Technology, UK) at an incident heat flux of 35 kW/m^2. Peak HRR, effective heat combustion (EHC), total heat evolved, specific extinction area (SEA), CO and CO_2 yield data are reproducible to within 10% tolerance when measured at 35 kW/m^2 flux.

2.6. Characterization of char surface

In this paper, we used SEM and ATR-IR spectra to characterize the char surface of the nanocomposite (OMMT mass fraction of 5 wt%) from start before ignition. SEM photographs of the char surface of the nanocomposite were taken on a Hitachi S-530 SEM. The surfaces were coated with gold and the accelerating voltage was 15 kV. The ATR-IR spectra were obtained on a Bruker TENSOR 27 FT-IR spectrometer equipped with an RT-DLaTGS ATR.

3. Results and discussion

3.1. Characterization of the composites

Fig. 1 shows the XRD patterns of clays (MMT and OMMT) and their composites with PA66 (MMT-5 and OMMT-5). The directly compounded MMT-5 revealed an unaltered *d*-spacing (1.23 nm), indicating that no polymer has entered the clay gallery. When using the organically modified MMT (OMMT, $d_{001} = 3.27$ nm), the characteristic (001) diffraction of the clay disappeared in the resultant OMMT-5. The absence of the (001) peak in the XRD pattern suggests that the clay has a nearly exfoliated effect in the PA66 matrix.

Fig. 2 shows the dispersion state of the composites observed by TEM. In MMT-5 (Fig. 2(A)), the primary particles composed of the aggregated silicate layers are observed in the polymer matrix, strongly suggesting an immiscible dispersion. On contrary, homogeneously exfoliated structure of the nanosized structural layers of the clay is present in OMMT-5 (Fig. 2(B)). The layered structure of the clay was still clearly observed under TEM at low magnification similar to Fig. 2(A).

Based on the XRD and TEM result, it is concluded that

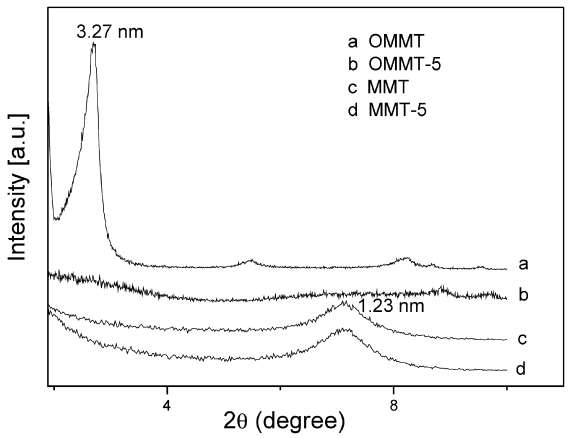

Fig. 1. XRD patterns of OMMT, OMMT-5, MMT and MMT-5.

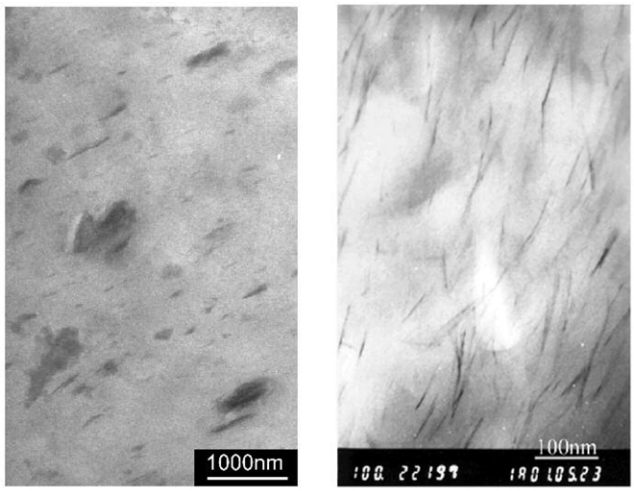

Fig. 2. TEM images of (A) MMT-5 and (B) OMMT-5.

PA66/OMMT is exfoliated nanocomposite and PA66/MMT is immiscible microcomposite.

3.2. Thermal stability

It is reported that some nanocomposites combined MMT and polymer matrix can improve thermal stability [11,12], such as poly(methyl methacrylate) (PMMA) [13], poly (dimethylsiloxane) (PDMS) [11], polyimide [14] and polypropylene [15]. The increase of thermal stability is attributed to hindered diffusion of volatile decomposition products within the nanocomposites [6].

The TGA curves of pure PA66, OMMT-5 nanocomposite and MMT-5 microcomposite in nitrogen and air environments are shown in Fig. 3. In both of ambient atmospheres, the nanocomposite has a higher decomposition temperature (434.2 °C in nitrogen and 447.8 °C in air) than the microcomposite (425.1 °C in nitrogen and 442.3 °C in air). The diversity reveals when compare to the pristine polymer: the decomposition temperature of the nanocomposite is 10 °C lower than the pure PA66 (445.8 °C) in nitrogen atmosphere but 7 °C higher than the pure PA66 (440.4 °C) in air atmosphere. The difference is due to the absence and the presence of oxygen. The thermal behaviour of the composite samples in nitrogen atmosphere indicates that the addition of MMT can accelerate the thermal decomposition of PA66 matrix. It is maybe due to the catalysis of water in MMT (bound or from dehydroxylation) [16]. In oxygen atmosphere, the degradation of the samples is mainly oxygenolysis and the barrier effect of the silicate layers is dominant due to the formation of carbonaceous silicate char on the surface of nanocomposite (the mechanism will be described later in this paper). Therefore, the composites have a higher thermal stability than pure PA66 in air.

The catalytic decomposition effect of MMT and the barrier effect of the silicate layers is much more evident in

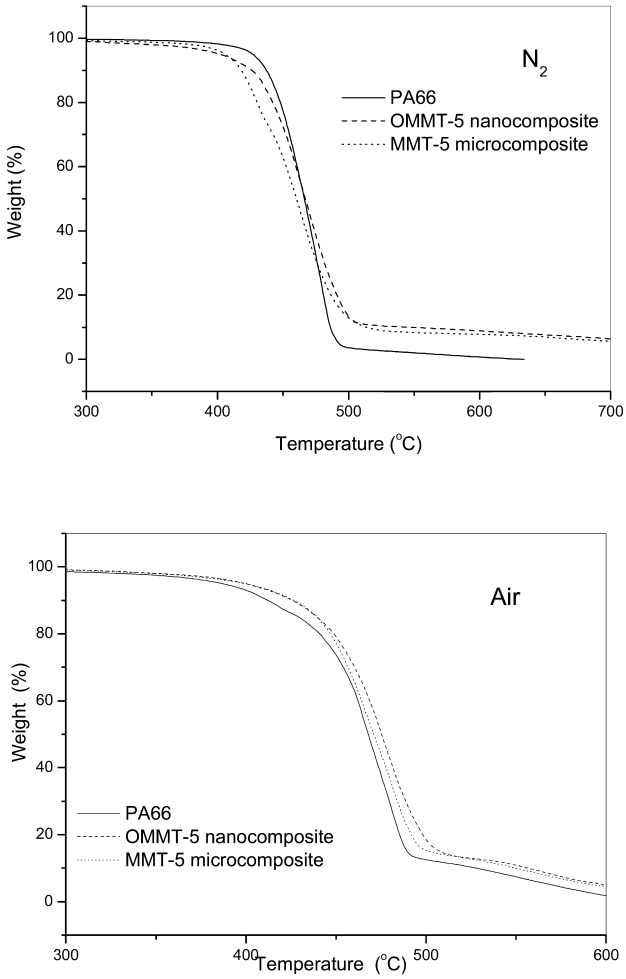

Fig. 3. TGA curves of pure PA66, OMMT-5 nanocomposite and MMT-5 microcomposite in different ambient atmospheres (TGA heating rate: 20 °C/min).

isothermal oxidation experiments as shown in Fig. 4. At 360 °C in air atmosphere, the volatilisation rate of either the nanocomposite or the microcomposite is faster than that of pure PA66 at the beginning; thereafter, the weight loss is

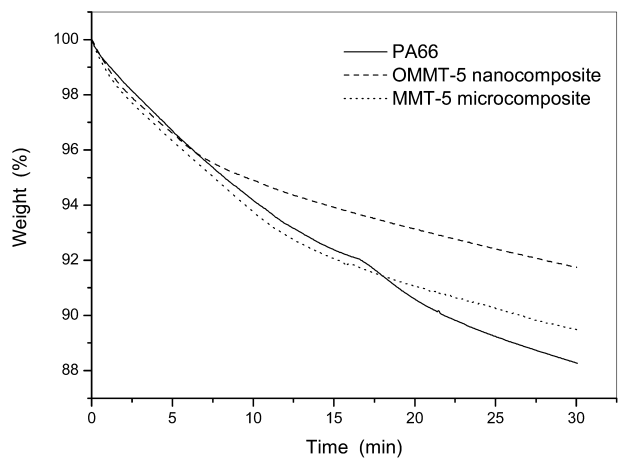

Fig. 4. Isothermal TGA curves of pure PA66, OMMT-5 nanocomposite and MMT-5 microcomposite (air atmosphere, 360 °C).

slowed down in both composites compared to the pure PA66 but with a large effect in the nanocomposite. It indicates that the nanocomposite has higher thermal stability than the microcomposite. This shows that the exfoliation of the silicate layers in polymer matrix can make the barrier effect more remarkable.

3.3. Combustion

The combustion properties of the PA66/clay composite were characterised by means of cone calorimetry. The HRR plots for OMMT-5 nanocomposite, MMT-5 microcomposite, and pure PA66 at 35 kW/m^2 heat flux are shown in Fig. 5. The peak HRR of the nanocomposite is 59% lower than that of pure PA66, which is typical of those reported in the literature [6–10]. The reduction in the peak HRR of the microcomposite is 32%. This indicates that the addition of MMT can decrease the HRR of PA66 matrix. The influence of the nanocomposite is more effective than that of the microcomposite. It is due to the barrier effect of the exfoliated nano-structure in the nanocomposite. As seen from the Fig. 5, the nanocomposite and the microcomposite have a shorter ignition time than pure PA66 and the initial HRR is higher for the first 100 s in the combustion. This is similar to the isothermal TGA curves of the samples in air. It is shown that the addition of MMT can accelerate the ignition of PA66 matrix. Perhaps it is due to the catalytic decomposition effect of MMT to polymer matrix.

Fig. 6 shows the MLR recorder during the cone calorimetric experiments. The MLR curves are identical to the HRR curves, so it is evident that the reduction of the MLR is the primary parameter responsible for the lower HRR of the composites.

The effect of varying OMMT loading in the nanocomposites on the HRR is shown in Fig. 7. The reduction in the peak HRR increases as the mass fraction of OMMT increases. Some cone calorimetric data of pure PA66 and composites are listed in Table 1. This reveals that the EHC,

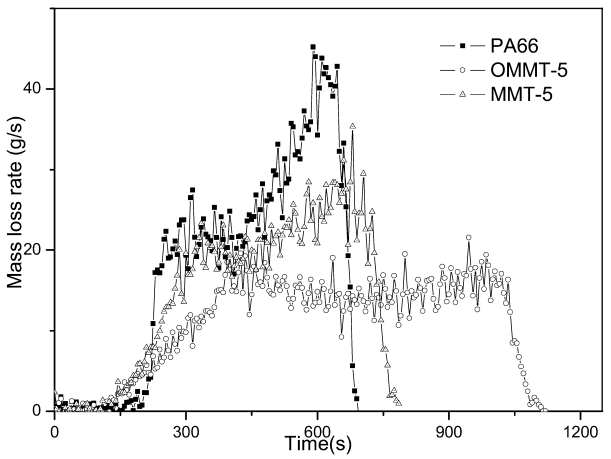

Fig. 6. MLR plots for pure PA66, OMMT-5 nanocomposite and MMT-5 nanocomposite, at a heat flux of 35 kW/m^2.

total heat evolved, average CO yield, and average CO_2 yield of composites are similar to those of pure PA66. Specific extinction area (SEA, a measure of smoke yield) of the nanocomposites have a 60% increase to that of pure PA66. This suggests that the source of the improved flammability of these materials is due to differences in condensed-phase decomposition processes and not to a gas-phase effect [6].

3.4. Characterization of char surface

In the cone calorimetric measurements, we observed that pure PA66 melted and had a boiling surface at the base of the flame, while the nanocomposite did not melt and a coat-like char formed in the surface. Although, the microcomposite did not melt, the char formed in the surface is flecky and discontiguous. At the end of combustion, pure PA66 left almost no residue, while the nanocomposite remained a voluminous char-like residue that kept the shape of the original specimen and the microcomposite a little char-like powder.

It was observed that the coat-like char formed in the

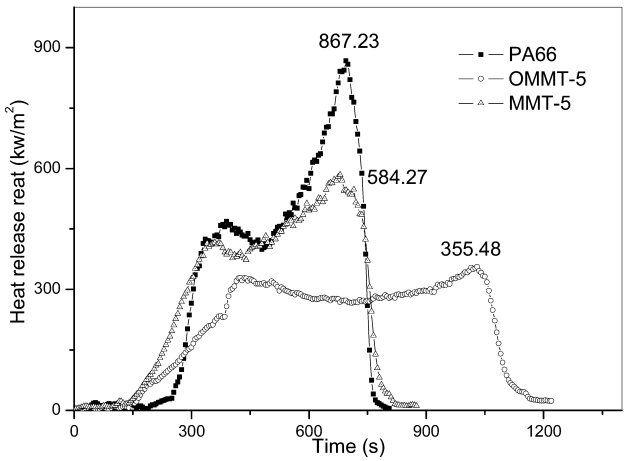

Fig. 5. Heat release rate (HRR) plots for pure PA66, OMMT-5 nanocomposite and MMT-5 microcomposite at a heat flux of 35 kW/m^2.

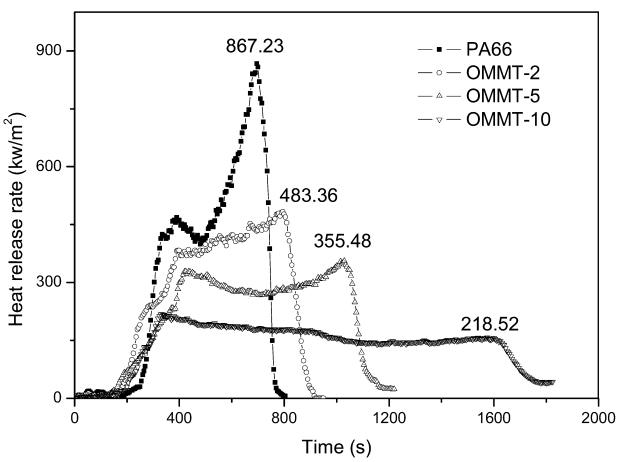

Fig. 7. Heat release rate (HRR) plots for pure PA66 and OMMT-2, OMMT-5, OMMT-10 nanocomposites at a heat flux of 35 kW/m^2.

Table 1
Data recorded in cone calorimeter experiments at a heat flux of 35 kW/m^2

Sample	PA66	OMMT-2	OMMT-5	OMMT-10	MMT-5
Peak HRR (kW/m^2)	802.4	496.1	335.5	209.4	537.8
Average EHC (MJ/kg)	0.18	0.18	0.19	0.19	0.19
Total heat evolved (MJ/m^2)	249.2	245.0	247.5	247.8	235.3
Average SEA (m^2/kg)	2.02	3.20	3.32	3.16	3.05
Average CO yield (kg/kg)	0.0001	0.0002	0.0002	0.0002	0.0001
Average CO_2 yield (kg/kg)	0.01	0.01	0.01	0.01	0.01
Ignition time (s)	169	163	139	152	127

surface of the nanocomposites from start before ignition. Fig. 8 shows the SEM micrograph of the char surface of the OMMT-5 nanocomposite under the state from start before ignition. The ceramic-like char surface is continuous and compact. It is like an overcoat to the nanocomposite and can significantly delay the rate of volatilisation of the nanocomposite and retard the penetration of oxygen.

ATR-IR spectra provide additional details of the coat-like char surface of the nanocomposite. Fig. 9 shows the ATR-IR spectra of the nanocomposite: the spectrum (A) was obtained from the surface of the nanocomposite from start before ignition and the spectrum (B) was obtained from the original surface of the moulded sample. The bands at 1083 and 1018 cm^{-1} are Si–O stretching of MMT. The bands at 1631 and 1533 cm^{-1} are the characteristic adsorption of PA66. Compared to the bands at 1631 and 1533 cm^{-1}, the bands of Si–O stretching have a dramatic increase after firing. It indicates that the carbonaceous silicate char forms in the surface of the nanocomposite, as soon as the nanocomposites are fired. It is an inorganic-rich surface that has better barrier property. As a result, the combustion of the nanocomposite hindered.

4. Conclusion

In this paper, PA66/OMMT nanocomposite and PA66/MMT microcomposite was prepared by melt processing. The composites have a higher thermal stability than pure PA66 in air, and the nanocomposite has a higher thermal stability than the microcomposite. In isothermal oxidation experiment, the catalytic decomposition effect of MMT and the barrier effect of silicate layers are presented directly. Combustion experiments show that the addition of MMT can decrease the HRR of PA66 matrix. The influence of the nanocomposite is more effective than that of the microcomposite. Moreover, the addition of MMT can accelerate the ignition of PA66 matrix. Perhaps it is due to the catalytic decomposition effect of MMT to polymer matrix. A ceramic-like char forms in the surface of the nanocomposite during burning. The characterization of the char surface from start before ignition indicates that it is an inorganic-rich surface that has better barrier property.

Acknowledgements

The work has been supported by the National 863 Programme (under the Grant number 2001AA334050) of the Ministry of Science and Technology of China. The authors would like to thank Prof. Zhongjun Shu and Prof. Shousheng Yang (Chinese People's Armed Police Force Academy) for their collaboration in cone calorimetric

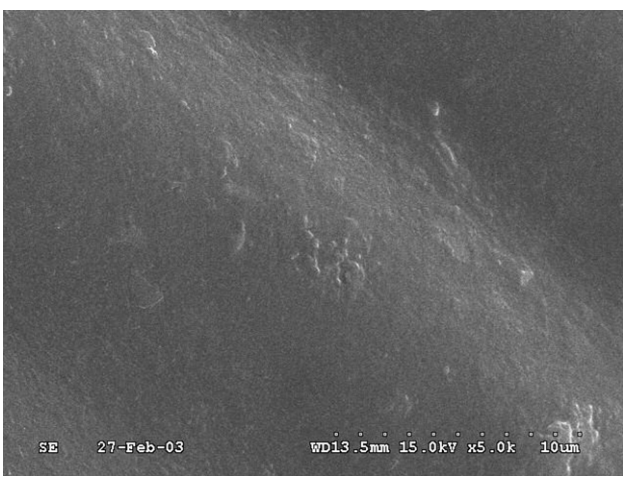

Fig. 8. SEM micrograph of the char surface of the OMMT-5 nanocomposite.

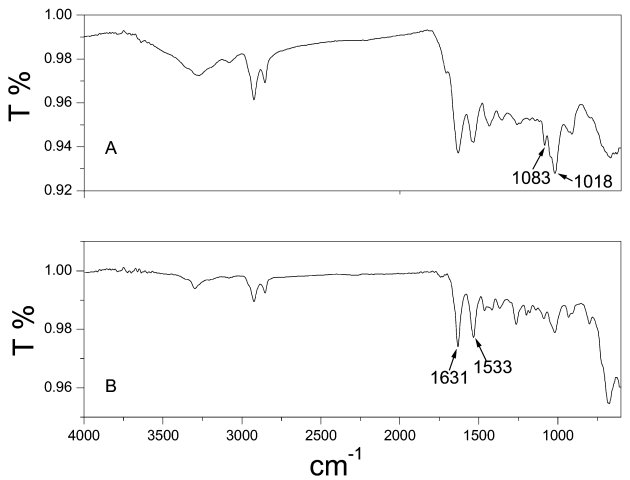

Fig. 9. ATR-IR spectra of OMMT-5 nanocomposite sample. (A) surface from start before ignition; (B) original surface.

experiments. Thanks also to Mr Gang Li and Ms Shijuan Chen for their assistance in sample preparation and ATR-IR analysis.

References

[1] Okada A, Kawasumi M, Kurauchi T, Kamigaito O. Polym Prepr 1987; 28:447.
[2] Giannelis EP. Adv Mater 1996;8:29.
[3] Garces JM, Moll DJ, Bicerano J, Fibiger R, McLeod DG. Adv Mater 2000;12:1835.
[4] Alexandre M, Dubios P. Mater Sci Engr: reports 2000;28:1.
[5] Kojima Y, Usuki A, Kawasumi M, Okada A, Fukushima Y, Kurauchi T, Kamigaito O. J Mater Res 1993;8:1185.
[6] Gilman JW, Jackson CL, Morgan AB, Harris R, Manias E, Gannelis EP, Wuthenow M, et al. Chem Mater 2000;12:1866.
[7] Gilman JW, Kashiwagi T, Lichtenhan J. SAMPE J. 1997;33:40.
[8] Gilman JW. Appl Clay Sci 1999;15:36.
[9] Zhu J, Uhl FM, Morgan AB, Wilkie CA. Chem Mater 2001;13:4653.
[10] Zanetti M, Kashiwagi T, Falqui L, Camino G. Chem Mater 2002;14: 883.
[11] Burnside SD, Giannelis EP. Chem Mater 1995;7:1597.
[12] Lee J, Takekoshi T, Giannelis EP. Mater Res Soc Symp Proc 1997; 457:513.
[13] Blumstein A. J Polym Sci 1965;A3:2665.
[14] Zhu ZK, Yang Y, Yin J, Wang XY, Ke YC, Qi ZN. J Appl Polym Sci 1999;73:2065.
[15] Zanetti M, Camino G, Peichert P, Mulhaupt R. Macromol Rapid Commun 2001;22:176.
[16] Davis RD, Gilman JW, VanderHart DL. Polym Degrad Stab 2003;79: 120.